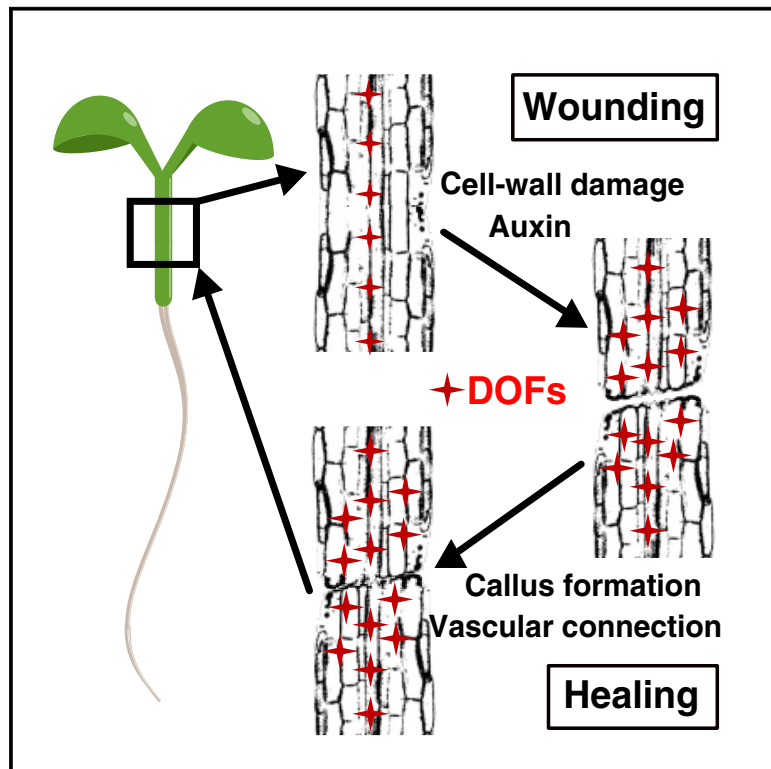# Cell-wall damage activates DOF transcription factors to promote wound healing and tissue regeneration in *Arabidopsis thaliana*

Graphical abstract

Authors

Ai Zhang, Keita Matsuoka,
Abdul Kareem, ..., Cătălin Voiniciuc,
Masashi Asahina, Charles W. Melnyk

Correspondence

charles.melnyk@slu.se

In brief

Plants require an efficient regeneration system to heal wounds. Zhang et al. identify four DOF transcription factors that are rapidly activated at sites of wounding, graft formation, or tissue cutting. These DOFs are activated by cell-wall damage and auxin to promote tissue regeneration and wound healing.

Highlights

- Four DOF transcription factors are rapidly activated at wounding and grafting sites

- Damage to or modifications of the cellulose and pectin matrix activate DOFs

- DOFs regulate callus formation, tissue adhesion, and vascular regeneration at wounds

- Wound-associated *ERF115* and *ANAC096* are also activated upon cell-wall damage

Current Biology

Article

Cell-wall damage activates DOF transcription factors to promote wound healing and tissue regeneration in *Arabidopsis thaliana*

Ai Zhang,[1] Keita Matsuoka,[2] Abdul Kareem,[1] Madalen Robert,[3] Pawel Roszak,[4] Bernhard Blob,[4] Anchal Bisht,[5,6] Lieven De Veylder,[5,6] Cătălin Voiniciuc,[3,7] Masashi Asahina,[2,8] and Charles W. Melnyk[1,9,10,*]

[1]Department of Plant Biology, Linnean Center for Plant Biology, Swedish University of Agricultural Sciences, Almas allé 5, 756 51, Uppsala, Sweden
[2]Department of Biosciences, Teikyo University, 1-1 Toyosatodai, Utsunomiya 320-8551, Japan
[3]Independent Junior Research Group – Designer Glycans, Leibniz Institute of Plant Biochemistry, 06120 Halle (Saale), Germany
[4]The Sainsbury Laboratory, University of Cambridge, Cambridge CB2 1LR, UK
[5]Department of Plant Biotechnology and Bioinformatics, Ghent University, 9052 Ghent, Belgium
[6]Center for Plant Systems Biology, VIB, 9052 Ghent, Belgium
[7]Horticultural Sciences Department, University of Florida, Gainesville, FL 32611, USA
[8]Advanced Instrumental Analysis Center, Teikyo University, 1-1 Toyosatodai, Utsunomiya 320-8551, Japan
[9]Twitter: @CharlesMelnyk
[10]Lead contact
*Correspondence: charles.melnyk@slu.se
https://doi.org/10.1016/j.cub.2022.02.069

SUMMARY

Wound healing is a fundamental property of plants and animals that requires recognition of cellular damage to initiate regeneration. In plants, wounding activates a defense response via the production of jasmonic acid and a regeneration response via the hormone auxin and several ethylene response factor (ERF) and NAC domain-containing protein (ANAC) transcription factors. To better understand how plants recognize damage and initiate healing, we searched for factors upregulated during the horticulturally relevant process of plant grafting and found four related DNA binding with one finger (DOF) transcription factors, *HIGH CAMBIAL ACTIVITY2* (*HCA2*), *TARGET OF MONOPTEROS6* (*TMO6*), *DOF2.1*, and *DOF6*, whose expression rapidly activated at the *Arabidopsis* graft junction. Grafting or wounding a quadruple *hca2, tmo6, dof2.1, dof6* mutant inhibited vascular and cell-wall-related gene expression. Furthermore, the quadruple *dof* mutant reduced callus formation, tissue attachment, vascular regeneration, and pectin methylesterification in response to wounding. We also found that activation of DOF gene expression after wounding required auxin, but hormone treatment alone was insufficient for their induction. However, modifying cell walls by enzymatic digestion of cellulose or pectin greatly enhanced *TMO6* and *HCA2* expression, whereas genetic modifications to the pectin or cellulose matrix using the *PECTIN METHYLESTERASE INHIBITOR5* overexpression line or *korrigan1* mutant altered *TMO6* and *HCA2* expression. Changes to the cellulose or pectin matrix were also sufficient to activate the wound-associated *ERF115* and *ANAC096* transcription factors, suggesting that cell-wall damage represents a common mechanism for wound perception and the promotion of tissue regeneration.

INTRODUCTION

Plants are commonly damaged, wounded, or fed upon, and they need to detect these injuries to initiate a successful repair response. Some of the earliest responses to wounding include changes in reactive oxygen species levels, calcium levels, turgor pressure, cell-wall integrity, hormones, and gene expression.[1–7] However, a common theme is that wounding induces a defense response to deter future damage, followed by a regeneration response to heal the wound and regrow tissues.[8] Such a system is exemplified during cutting or insect feeding when jasmonic acid levels increase within several minutes of wounding to active defense responses and suppress growth.[9] Continuous jasmonic acid treatment is inhibitory to regeneration, yet short jasmonic

acid treatments increase synthesis of the hormone auxin via the transcription factor *ETHYLENE RESPONSE FACTOR109* (*ERF109*) to allow successful regeneration of *de novo* roots.[10] At the wound site, auxin accumulates by both local biosynthesis and long-distance apical transport, where it activates cell division and cell differentiation.[6,10–12] Auxin accumulation upregulates several transcription factors, including *NAC DOMAIN-CONTAINING PROTEIN071* (*ANAC071*) and *ANAC096*, that promote cell divisions and cell-wall remodeling.[11,13–15] Several other transcription factors are also upregulated by wounding, including *ERF115* that normally regulates cell divisions in the quiescent center (QC) but whose expression expands to the site of wounding after cellular damage from bleomycin, cutting, or cell ablation.[7,12,16] *ERF115* expression also increases when

plants are treated with H_2O_2, brassinosteroids, auxin, or jasmonic acid, suggesting that multiple hormones and signals regulate wound response.[16–18] Blocking ERF and ANAC function impairs regeneration; for instance, dominant-negative *ERF115-SRDX* seedlings display impaired root tip regeneration, whereas dominant-negative *ANAC071-SRDX* and *ERF113-SRDX* plants fail to heal stem cuts.[11,19]

Wound responses include changes to cell-wall structure and recognition of cell-wall damage. Wounding typically induces anisotropic cell growth to fill the wound, and this directional growth results from modifications to pectin biochemistry and cellulose orientation.[20–22] Cell swelling characteristic of wounding is also found in mutants and isoxaben-treated plants that are cellulose deficient.[23,24] However, to date, the role of cell-wall damage has primarily been associated with defense responses. Cell-wall breakdown products, such as oligogalacturonides and cellodextrins derived from wounded tissues or pathogen attack, suppress growth and trigger defense responses.[25,26] Levels of the defense hormone jasmonic acid increase upon isoxaben treatment and in the cellulose-deficient *korrigan1* (*kor1*) mutant.[4,27] Since jasmonic acid signaling in wounded tissues is reduced by sorbitol or mannitol treatment,[27] turgor pressure is thought to also play a role in wound perception. The role of cell-wall damage upon regeneration is poorly understood, but here, too, cell-wall modifications likely play a role, since mannitol treatment inhibits *ERF115* induction,[7] whereas modifying pectins via *PECTIN METHYLESTERASE INHIBITOR5* overexpression increases auxin responses in hypocotyls.[28]

Recently, a role for auxin and cell-wall modifications was reported during the process of grafting when two plants are cut and joined together.[29] Successful grafting requires the formation of callus, an undifferentiated stem-cell-like tissue, to attach the tissues followed by vascular differentiation to reform phloem and xylem connections.[30] Adding auxin or cellulase promoted graft attachment that could be enhanced further when both chemicals were added.[29] Thousands of genes are induced during grafting, including those associated with auxin signaling and cell-wall biogenesis.[31] Auxin also plays an important role since auxin responses increase at the graft junction, and mutants in auxin signaling block graft junction healing.[21] Although cell-wall dynamics during graft healing remain largely uncharacterized, it is known that pectins are deposited at the graft junction, and induction of the *GH9B3* putative cellulase is important to graft *Nicotiana* with distantly related species.[30,32] Auxin is likely involved in early wound recognition, and some of the earliest genes activated during graft formation include several DNA binding with one finger (DOF) transcription factors of which at least one, *HIGH CAMBIAL ACTIVITY2* (*HCA2*), is auxin inducible and modifies graft healing.[31] Other DOFs have also been implicated in regeneration since *DOF5.4/OBP4* promotes callus formation.[33] However, how these early-acting transcription factors are activated and the mechanistic details for how auxin and cell walls activate regeneration remains unclear.

Here, we build upon our previous observations regarding auxin signaling and early grafting transcriptional responses to explore the biological relevance of these genes and the processes that regulate them. We identify a group of four DOF transcription factors and propose that cell-wall modifications activate these wound response regulators to promote tissue regeneration.

RESULTS

Four DOFs are important for grafting and wound response

Our previous work revealed that two DOF transcription factors, *HCA2* and *TARGET OF MONOPTEROS6* (*TMO6*), were activated early during graft formation and one, *HCA2*, contributed to healing.[31] We investigated the grafting transcriptome further and found that multiple DOF transcription factors were differentially expressed by wounding, including the *PEAR1*, *PEAR2*, *OBP1*, and *OBP4* genes associated with procambium formation or cell cycle (Figures S1A and S1B).[33–35] However, four DOF genes were exceptional since *HCA2*, *TMO6*, *DOF2.1*, and *DOF6* were induced within 6 h of wounding and formed their own sub-clade in a phylogenetic tree (Figures S1A and S1C), suggesting that these related proteins might share a common function. Transcriptional reporters confirmed that all four genes were activated at the graft junction within 12 h of grafting (Figures 1A–1D). Their expression increased in the vascular tissues and, for *TMO6* and *HCA2*, also spread into outer cell layers (Figures 1E, 1F, S1D, and S1E). To better understand the function of these related DOFs, we tested loss-of-function mutants but found no effects on phloem reconnection at the graft junction with single, double, or triple mutants (Figure S1F). However, grafting with the quadruple mutant, *hca2, tmo6-4, dof2.1-1, dof6-1*, which we termed the dofQ mutant, reduced tissue attachment, phloem reconnection, xylem reconnection, and root growth after grafting (Figures 1G–1I and S1G). Mutating these genes either above or below the graft junction inhibited phloem reconnection, though inhibition was strongest when *HCA2*, *TMO6*, *DOF2.1*, and *DOF6* were mutated in both locations (Figure S1H). Overexpression of *HCA2*, *TMO6*, *DOF2.1*, or *DOF6* below the graft junction accelerated the rate of phloem reconnection (Figures S1I and S1J), demonstrating that DOF levels could modulate the healing response. Grafting encompasses several aspects of wound healing, including tissue attachment, callus formation, and vascular regeneration.[30] To look at these individual processes, we used confocal laser ablation to kill cells in the hypocotyl or root vascular tissue and found a strong upregulation of *TMO6*, *HCA2*, *DOF2.1*, and *DOF6* fluorescent reporters in the vascular tissues surrounding the wound (Figure 2A; Video S1). *TMO6pro:erRFP* and *HCA2pro:erRFP* also showed expanded fluorescence into the endodermis and cortex, similar to what we observed at the graft junction (Figures 1E, S1D, and 2A). Ablating cells in the cortex region also caused *TMO6* and *HCA2* upregulation at the site of wounding and in the surrounding cells (Figure 2B). We also looked at the effect resulting from inflorescence cutting or hypocotyl pinching with forceps and found DOF upregulation during both processes (Figures S2A–S2C). This DOF induction appeared relevant, since the dofQ mutant showed impaired wound healing after inflorescence cutting (Figure 2C). The dofQ mutant also reduced callus formation in cut petioles or cut hypocotyls, whereas overexpressing *TMO6* increased callus formation in both tissues (Figures 2D and S2D–S2F). Notably, the dofQ mutant exhibited no substantial changes in plant morphology or primary root development (Figures S2G–S2I). Together, these results suggested that the DOF genes were induced early after wounding and played an important role in wound healing and graft regeneration.
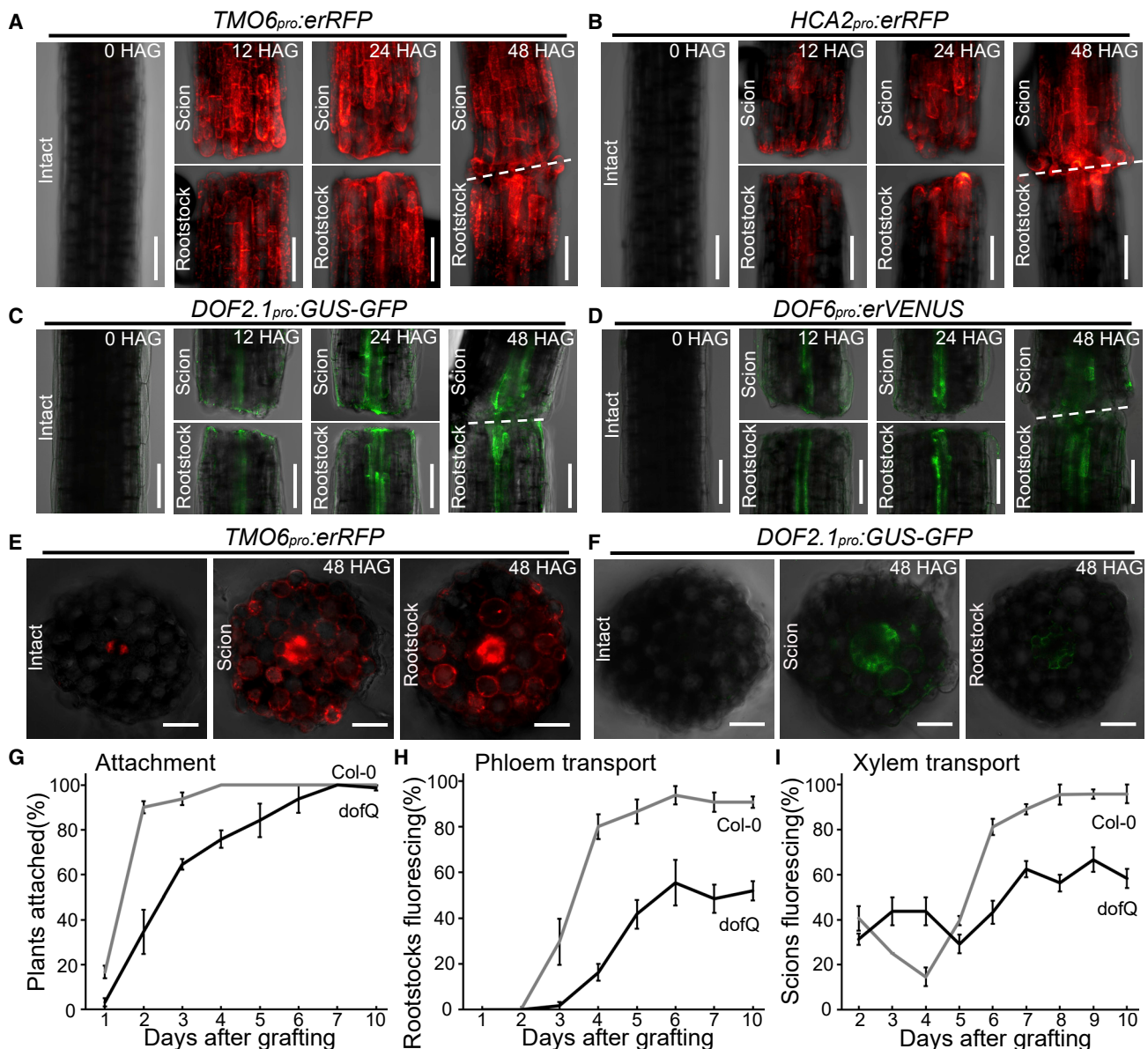
Figure 1. DOFs are required for successful graft formation

(A–D) *TMO6pro:erRFP*, *HCA2pro:erRFP*, *DOF2.1pro:GUS-GFP*, and *DOF6pro:erVENUS* are upregulated 12–48 h after grafting (HAG). The gap or dashed line indicates the graft junction. Scale bar, 100 μm.

(E and F) Transverse hand sections from intact and grafted *TMO6pro:erRFP* and *DOF2.1pro:GUS-GFP* at 48 HAG. Scale bar, 50 μm.

(G) Attachment rates of wild type and the dofQ mutant 1–10 days after grafting. The mean ± SEM from five experiments with 12–16 plants per time point per experiment is shown.

(H) Phloem reconnection of wild type and the dofQ mutant 1–10 days after grafting. The mean ± SEM from five experiments with 12–16 plants per time point per experiment is shown.

(I) Xylem reconnection of wild type and the dofQ mutant 2–10 days after grafting. The mean ± SEM from three experiments with 15–16 plants per time point per experiment is shown.

See also Figure S1.

DOFs modify cell-wall composition and are induced by changes to pectin and cellulose

To understand how *TMO6, HCA2, DOF2.1*, and *DOF6* affected graft healing, we performed a transcriptome analysis of the dofQ mutant. Genome-wide transcript levels were measured above and below the graft junction 24 h after grafting and also in intact (uncut) hypocotyls. We identified several hundred genes that showed differential expression in the dofQ mutant compared with wild type during graft healing (Figures 3A and S3A; Data S1). Cambium-related (e.g., *RUL1* and *ARF5*) and phloem-related (e.g., *BAM3* and *CLERK*) genes had a lower induction in dofQ (Figures 3B, 3C, and S3B). A large number of cell-wall-related
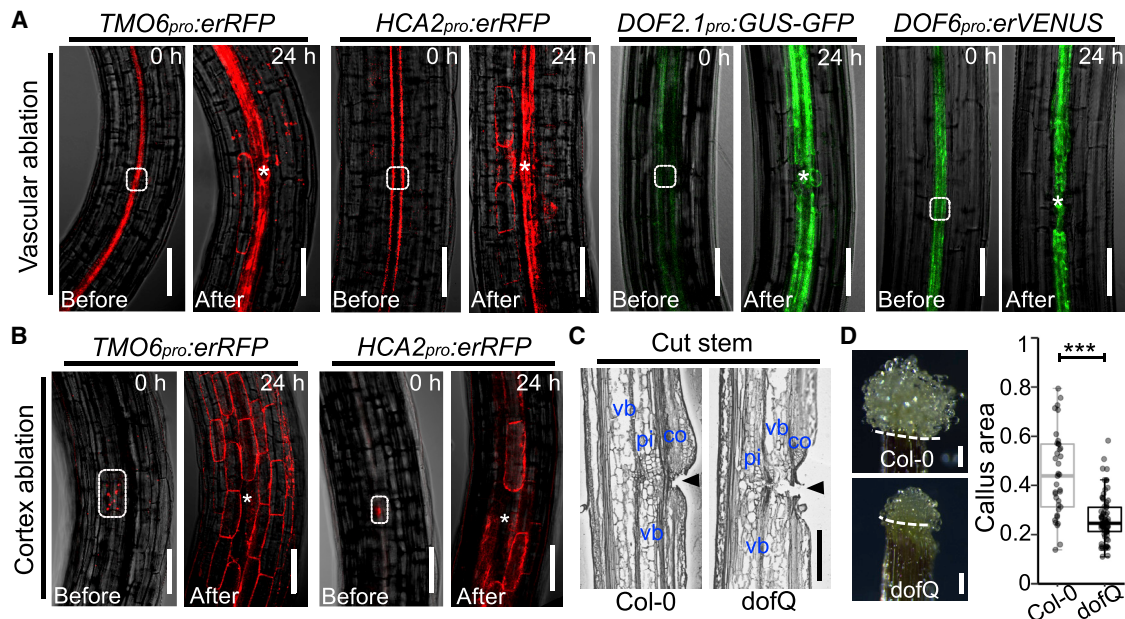
Figure 2. DOFs are wound responsive and important for regeneration

(A) Laser ablation of vascular cells of hypocotyl tissues upregulated *TMO6pro:erRFP*, *HCA2pro:erRFP*, *DOF2.1pro:GUS-GFP*, and *DOF6pro:erVENUS* expression in vascular cells above and below the wound site at 24 h after ablation. Also note ectopic upregulation of *TMO6pro:erRFP* and *HCA2pro:erRFP* expression in cortex cells after vascular cell ablation. The white dotted box and asterisks denote the ablation sites at 0 and 24 h, respectively.

(B) Laser ablation of hypocotyl cortex cells upregulated *TMO6pro:erRFP* and *HCA2pro:erRFP* expression in cortex and epidermal cells at 24 h after ablation. The white dotted box and asterisks denote the ablation sites at 0 and 24 h, respectively.

(C) Representative cryosection of Col-0 or dofQ flowering stems at 7 days after incision. Black arrowheads indicate position of cut. pi, pith; co, cortex; vb, vascular bundle. Scale bars, 500 μm.

(D) Representative images of callus formation at wound sites of wild-type and dofQ petiole explants. Dashed lines indicate the cut site. Scale bar, 100 μm. Boxplots represent the distribution of projected callus area of wild-type and dofQ petiole explants. Dots indicate individual data points (n = 37 plants for Col-0, 72 for dofQ). Asterisks indicate statistically significant differences compared with Col-0 (Wilcoxon test; ***p < 0.001).

See also Figure S2 and Video S1.

genes were not induced as highly in the dofQ mutant compared with wild type, particularly in the grafted rootstock (Figure 3D; Table S1). *CELLULASE3 (CEL3/GH9B3)*, previously implicated in inter-species graft formation,[32] was one such gene and could be a direct target of the DOFs, since TMO6 bound the *CEL3* promoter based on ChIP qPCR (Figures 3C and S3C). Grafting with a *cel3-2* mutant delayed phloem and xylem reconnection rates (Figures S3D and S3E). Other cell-wall-related genes, including members of the pectin methyl esterase (PME) family,[36] were upregulated, since we found that six PMEs were increased in the dofQ rootstock compared with wild type after grafting (Figure S3F). To evaluate how the cell walls of dofQ seedlings were impacted, analyses of cell-wall polysaccharides revealed reduced levels of rhamnose, increased levels of arabinose, and a slightly higher degree of methylesterification (DM) for pectins compared with wild type (Figures 3E, 3F, and S3G). Consistent with these biochemical changes, ruthenium red staining of low DM pectins showed reduced intensity for dofQ mutant roots compared with wild type (Figure S3H). After wounding, the cell-wall composition of wild-type seedlings contained multiple changes, including decreased D-galacturonic acid (GalA), increased pectin DM, and a slight, but not statistically significant, increase in crystalline cellulose content (Figures 3E, 3F, S3G, and S3I). However, unlike the wild type, wounding of the dofQ mutant increased its GalA content but did not alter its pectin DM

(Figures 3E and 3F). Furthermore, dofQ seedlings were hypersensitive to pectinase or cellulase treatments when these wall-degrading enzymes were included in the growth media (Figure S3J). Together, these data indicate that the dofQ mutant was perturbed in its cell-wall composition and that DOF genes were required for wound-induced pectin modifications.

Our previous results using cut and separated hypocotyls showed that *HCA2* was activated above the cut but not below it.[31] We confirmed this observation for *HCA2* and found that *TMO6* behaved similarly (Figures 4A and S1A) and reasoned that such asymmetry would allow us to investigate signals that activate DOFs. Plant wounding is known to induce cell-wall damage;[37] therefore, we investigated whether cell-wall changes affected DOF expression. Cut hypocotyls treated with Driselase, an enzymatic cocktail that degrades a wide range of plant wall polysaccharides,[4] activated *TMO6pro:erRFP* expression above and below the cut in separated hypocotyls and activated *HCA2pro:erRFP* below the cut in separated hypocotyls (Figures S4A–S4D). Treatments with cellulase or pectinase similarly activated *TMO6pro:erRFP* and *HCA2pro:erRFP* in cut tissues, but not intact tissues, suggesting that pectin or cellulose degradation enhanced DOF expression (Figures 4A and S4B–S4F). Treatments with salicylic acid or jasmonic acid, two stress-associated hormones, have no effect upon *TMO6* induction (Figures S4A and S4B). To investigate this phenomenon
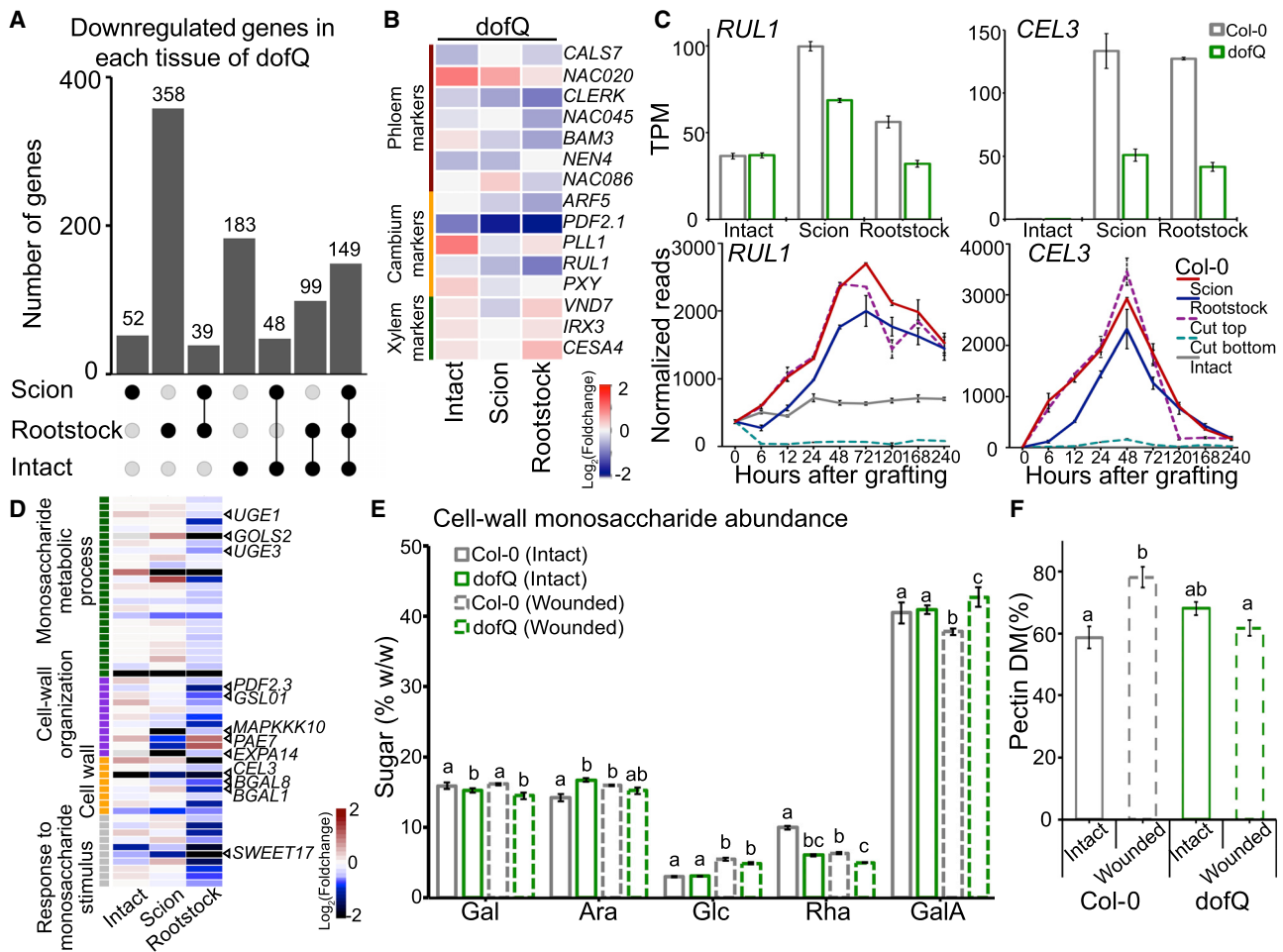
Figure 3. DOFs regulate cell-wall-related genes during regeneration

(A) UpSet plot displaying the intersecting sets of downregulated genes in the scion, rootstock, and intact tissues of dofQ compared with Col-0 at 24 h after grafting.

(B) Expression differences of various vascular marker genes in intact, scion, or rootstock tissues of dofQ compared with Col-0 at 24 h after grafting.

(C) Expression profiles for *RUL1* and *CEL3*. Histogram plots represent transcripts per million (TPM) values for genes of interest in the dofQ mutant at 24 h after grafting. Line plots represent the expression levels of genes of interest for grafted, cut, and intact samples. Line plot grafting RNA-seq values from Melnyk et al.[31]

(D) Heatmap showing differentially expressed genes in the dofQ mutant compared with Col-0 at 24 h after grafting. Genes were selected based on downregulation in the scion or rootstock tissues (q < 0.05) and containing cell-wall-related GO terms.

(E) Cell-wall monosaccharide composition analysis from intact and wounded Col-0 and dofQ at 48 h after wounding. Values represent mean ± SD of three replicates. Gal, galactose; Ara, arabinose; Glc, glucose; Rha, rhamnose; GalA, galacturonic acid. Additional monosaccharide levels are listed in Figure S3F. p value was calculated by ANOVA followed Tukey's HSD test. Letters indicate statistically significant differences.

(F) Degree of methylesterification (DM) for pectin in intact and wounded Col-0 and dofQ at 48 h after wounding. The values represent mean ± SD of three replicates. p value was calculated by ANOVA followed Tukey's HSD test. Letters indicate statistically significant differences.

See also Figure S3, Table S1, and Data S1.

genetically, we used two genotypes perturbed in cell wall composition. The *PMEI5* overexpression line *35S_pro:PMEI5* (*PMEI5oe*) has increased pectin DM, reduced cell expansion, and increased cell stiffness in the hypocotyl,[28,38] whereas the *korrigan1* mutant impairs cellulose biosynthesis and has increased cell expansion.[27,39,40] The *PMEI5oe* line increased *TMO6* and *HCA2* transcript levels in intact and wounded plants, accompanied by enhanced phloem reconnection rates (Figures 4B and 4C). Introducing the negative repressor *HCA2-SRDX*[41] into the *PMEI5oe* background reduced the enhanced phloem reconnection of *PMEI5oe* (Figure S4G). Consistent with

HCA2 acting downstream of PMEIs, the overexpression line *hca2-OE*[41] in the *PMEI5oe* background grafted similar to *PMEI5oe* or *hca2-OE* alone (Figure S4H). On the other hand, the *kor1* mutant decreased *TMO6*, *HCA2*, and *DOF2.1* transcript levels in wounded hypocotyls and reduced xylem reconnection rates (Figures 4D, 4E, S4I, and S4J). However, *kor1* did not seem to significantly impact phloem reconnection (Figure S4K). Mannitol treatments have been previously shown to reduce turgor pressure and wound response,[7,27] and we also observed a reduction in DOF activation upon mannitol treatment, but this effect could be rescued by Driselase treatment
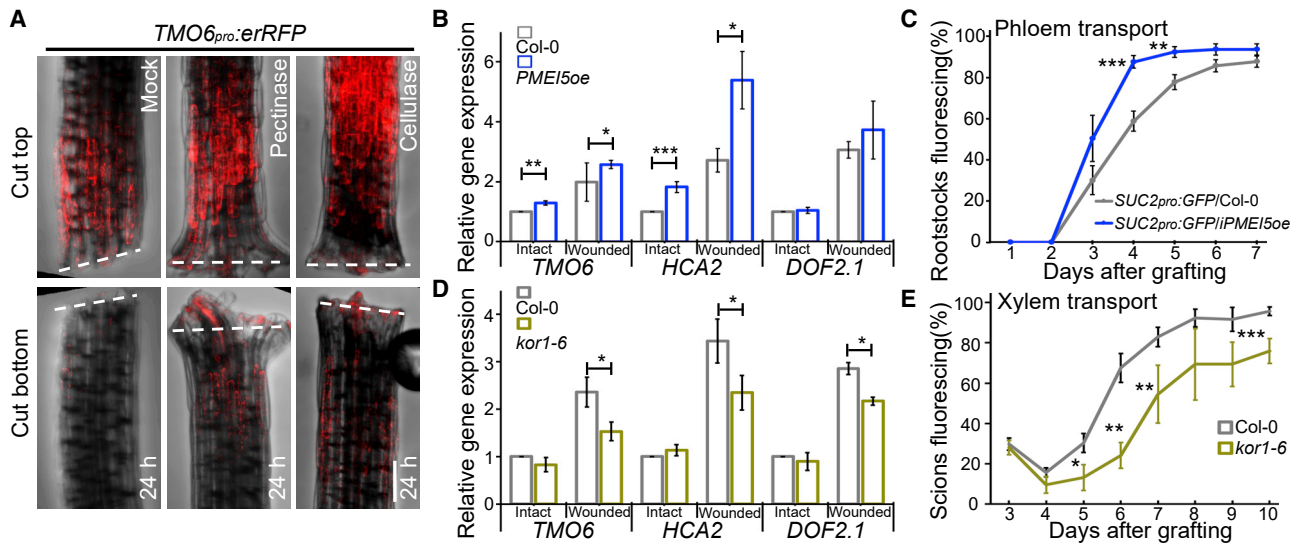
Figure 4. Cell-wall modifications induce DOF expression

(A) Response of cut hypocotyl tops and bottoms expressing *TMO6pro:erRFP* under various treatments after 24 h. Pectinase, 0.03%; cellulase, 0.03%. Dashed lines indicate the cut sites. Scale bar, 100 μm.

(B) Relative expression levels of *TMO6*, *HCA2*, and *DOF2.1* in intact or forceps wounded *PMEI5oe* after 24 h of wounding. Values are normalized by *PP2A* expression and represent the mean ± SEM of four experiments (n = 45–60 plants per experiment). Asterisks indicate statistically significant differences compared with indicated Col-0 (Student's t test; *p < 0.05; **p < 0.01; ***p < 0.001).

(C) *SUC2pro:GFP* Col-0 scions were grafted to Col-0 or inducible *PMEI5* overexpression line (*iPMEI5oe*) rootstocks and phloem reconnection monitored from 1 to 7 days after grafting and estradiol induction. The mean ± SEM from six experiments with 9–11 plants per time point per experiment is shown. Asterisks indicate statistically significant differences compared with Col-0 (Student's t test; **p < 0.01; ***p < 0.001).

(D) Relative expression levels of *TMO6*, *HCA2*, and *DOF2.1* in intact or forceps wounded *kor1-6* after 24 h of wounding. Values are normalized by *PP2A* expression and represent the mean ± SEM of three to four experiments (n = 45–60 plants per experiment). Asterisks indicate significant differences compared with indicated Col-0 (Student's t test; *p < 0.05).

(E) Xylem reconnection of the *kor1-6* mutant 3–10 days after grafting. The mean ± SEM from three experiments with 15–16 plants per time point per experiment is shown. Asterisks indicate significant differences compared with Col-0 (Student's t test; *p < 0.05; **p < 0.01; ***p < 0.001).

See also Figure S4.

(Figures S4A–S4D). Together, these data demonstrate that cellulose- and pectin-based modifications to the cell wall were sufficient to activate DOF expression in intact and wounded plants.

Auxin contributes to DOF activation

Auxin plays an important role in wound healing, and previously, we found that exogenous auxin induced *HCA2* in cut hypocotyls.[31] We confirmed this finding and also found that exogenous auxin (NAA) activated *TMO6pro:erRFP* in cut hypocotyls (Figures 5A, 5B, and S5A–S5D). In untreated plants, activation of *HCA2* and *TMO6* was much stronger above the cut than below the cut when plants were left separated (Figures 5A and S5A), suggesting a mobile substance, such as sugar or auxin, could be responsible for the asymmetric expression pattern of *HCA2* and *TMO6*. Exogenous sugar treatment had no effect on DOF induction, but blocking auxin transport with NPA or blocking auxin receptors with auxinole greatly reduced *TMO6pro:erRFP* and *HCA2pro:erRFP* expression at the cut site (Figures 5A, 5B, and S5A–S5E), suggesting that shoot-derived auxin was necessary for *TMO6* and *HCA2* induction. We investigated the genetic requirements for auxin by testing various auxin-related mutants for changes in DOF levels. Most had little effect; however, the expression of *TMO6*, *HCA2*, and *DOF2.1* was inhibited in the *iaa18-1* dominant mutant that blocks auxin

signaling[42] and inhibits graft formation,[21] suggesting that auxin signaling is required for their transcriptional activation (Figures 5C and S5G–S5I). Overexpressing *TMO6* or *HCA2* in the *iaa18-1* mutant background partially rescued phloem reconnection at the graft junction rootstock in *SUC2pro:GFP* assays (Figure 5D), suggesting that enhanced DOF expression could compensate for a lack of auxin signaling. *HCA2* and *TMO6* have not been previously described as auxin responsive,[35,41,43] and treating intact *TMO6pro:erRFP* and *HCA2pro:erRFP* plants with auxin did not change fluorescence levels (Figure S5F), indicating that wounding was required for auxin enhancement. We therefore investigated whether cell-wall damage might be a wound signal that contributes to auxin-induced DOF activation. We combined chemical treatments but found that adding auxin to cellulase or pectinase was not additive for *TMO6pro:erRFP* intensity (Figures 5A, 5B, S5A, and S5B). However, the inhibiting effects of auxinole could be modified by cell-wall digestion (Figures 5A, 5B, S5A, and S5B). Auxinole combined with cellulase showed strong *TMO6pro:erRFP* induction similar to cellulase treatment alone, whereas auxinole combined with pectinase showed little *TMO6pro:erRFP* induction (Figures 5A, 5B, S5A, and S5B). Thus, it appeared that degrading pectins could not overcome auxin receptor inhibition but degrading cellulose could. We investigated this aspect genetically by generating the
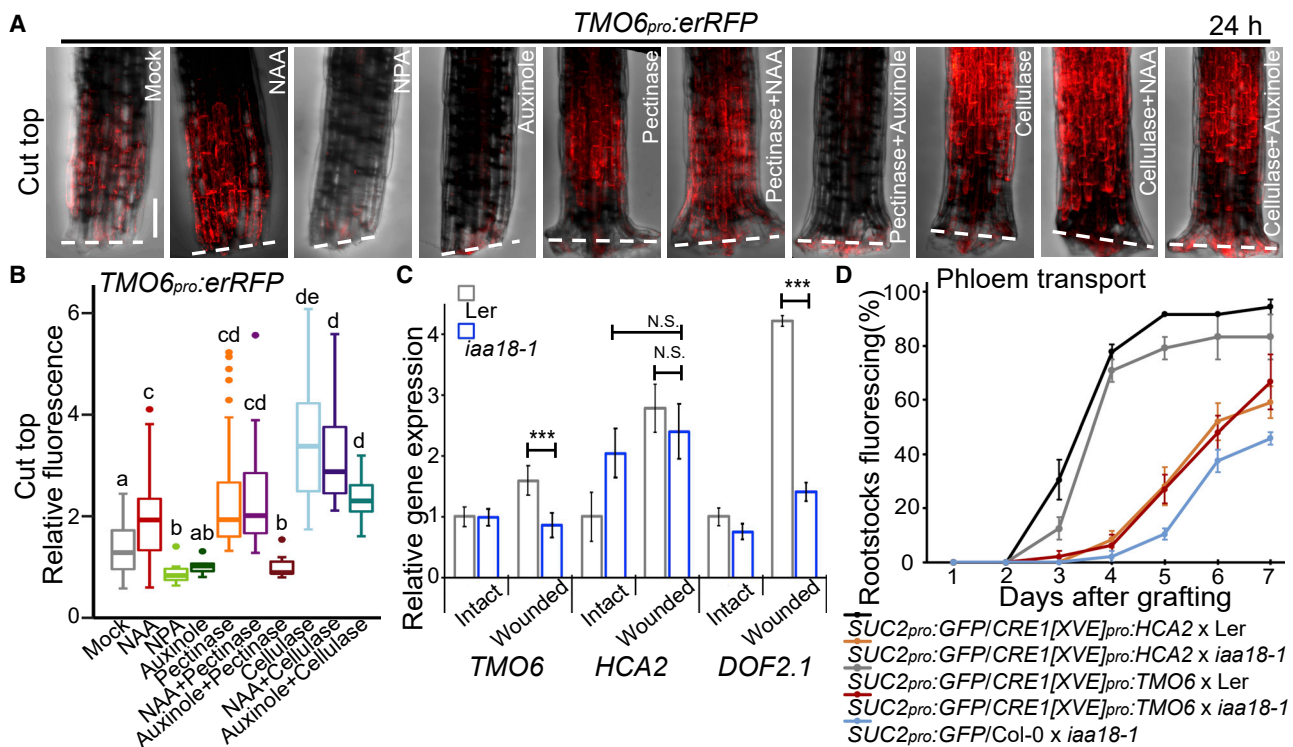
Figure 5. Auxin is important for DOF induction

(A) Cutting response of hypocotyl tops expressing *TMO6pro:erRFP* under various treatments after 24 h. NAA, 0.2 µM; NPA, 5 µM; auxinole, 30 µM; pectinase, 0.03%; cellulase, 0.03%. The dashed line denotes the cut site. Scale bar, 100 µm.

(B) Quantification of the intensity of *TMO6pro:erRFP* under various treatments after 24 h in (A). n = 96 plants for mock, 45 for NAA, 6 for NPA, 5 for auxinole, 9 for pectinase + NAA, 8 for pectinase + auxinole, 9 for cellulase + NAA, and 16 for cellulase + auxinole. p value was calculated by Wilcoxon test with all pairwise comparisons. Letters indicate statistically significant differences.

(C) Relative expression levels of *TMO6*, *HCA2*, and *DOF2.1* in intact or forceps wounded *iaa18-1* after 24 h of wounding. Values are normalized by *PP2A* expression and represent the mean ± SEM of five experiments (n = 45–55 plants per experiment). Asterisks indicate statistically significant differences compared with indicated plants (Student's t test; ***p < 0.001). N.S. represents no statistical significance.

(D) *SUC2pro:GFP* Col-0 scions were grafted to rootstocks of indicated genotypes and phloem reconnection monitored from 1 to 7 days after grafting and estradiol induction. F1 plants from a cross of the indicated genotypes on the figure were analyzed. Plants containing the *iaa18-1* mutation are from a heterozygous population. The mean ± SEM from three to six experiments with 11–12 plants per time point per experiment is shown.

See also Figure S5.

PMEI5oe iaa18-1 mutant and found indeed that it grafted similar to the *iaa18-1* mutant (Figure S5J), consistent with pectin modifications requiring auxin signaling for wound induction.

Wound-induced ERFs and ANACs also respond to changes in pectin and cellulose

ANAC and ERF transcription factors are important regulators of wound healing.[11,16] Investigating our previously published grafting transcriptome in greater detail revealed the rapid induction of *ERF114*, *ERF115*, *ANAC071*, and *ANAC096*, which we could confirm with transcriptional reporter activation after grafting or wounding (Figures 6A, 6B, S6A, and S6B). We generated a mutant between *ERF115* and its close homolog *ERF114* and tested *erf114,115* along with a previously published *anac071,096* mutant.[14] As a result, we found reduced callus formation and delayed phloem reconnection similar to the *dofQ* mutant (Figures 6C and S6C–S6E). To understand how these genes affect regeneration, we performed an RNA-seq

transcriptome analysis of *erf114,115* and *anac071,096* and found substantial changes during graft healing (Figures S6F and S6G; Data S2 and S3). Compared with wild type, *anac071,096* reduced phloem- and cambium-related gene induction, whereas *erf114,115* reduced xylem-, phloem-, and cambium-related gene induction (Figure S6H).

Our previous results demonstrated that pectin and cellulose modifications activated DOFs; therefore, we tested whether cell walls might play a similar role with wound-induced ERFs and ANACs. In the grafting transcriptome, we found that multiple cell-wall-related genes were downregulated in the *erf114,115* and *anac071,096* mutants, including *CEL3* (Figure 6D). Treating *ERF115pro:GUS-GFP* with cellulase, pectinase, auxin, or a combination of these induced *ERF115pro:GUS-GFP* expression in intact roots (Figure 6E). Auxin signaling appeared important, since *iaa18-1* was sufficient to block *ERF115pro:GUS-GFP* expression at the graft junction (Figure S6I). Notably, treatments with auxin and cell-wall-degrading enzymes appeared additive for *ERF115pro::GUS-GFP*, unlike the situation with *TMO6pro:erRFP*
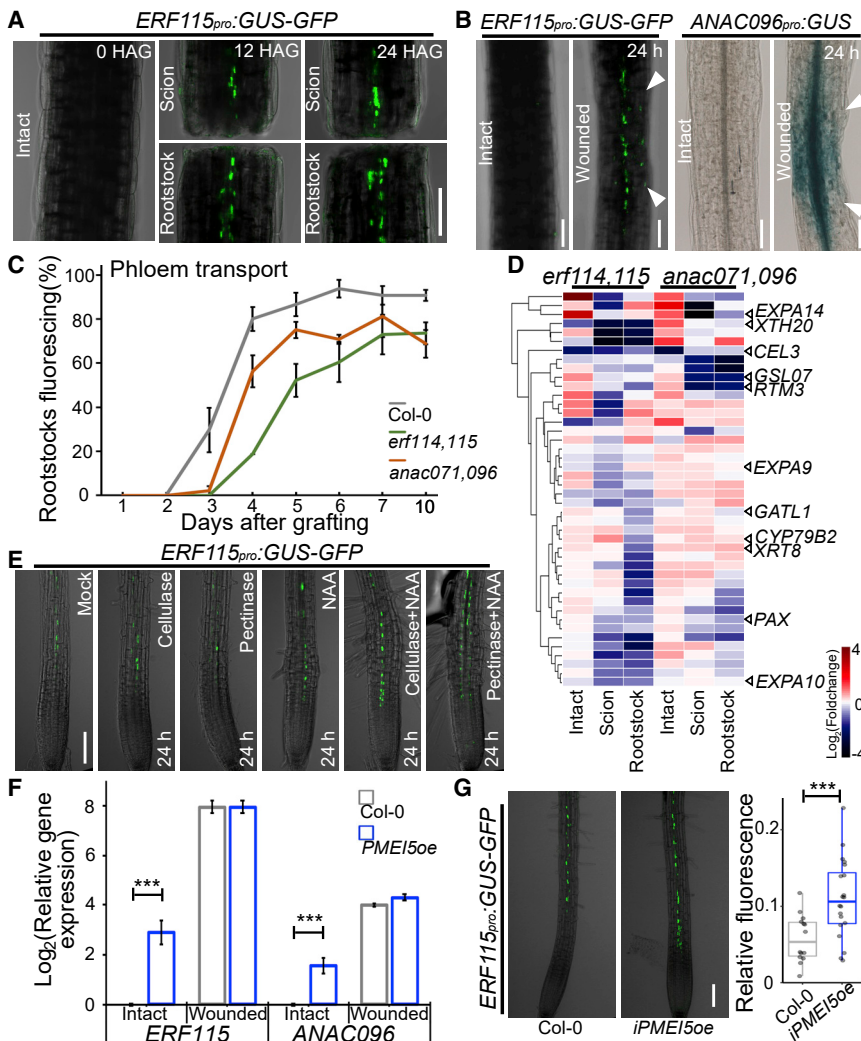
Figure 6. Cell-wall modifications induce *ERF115* and *ANAC096* expression

(A) *ERF115* is upregulated 12–24 h after grafting (HAG). The gap indicates the graft junction. Scale bar, 100 μm.

(B) *ERF115* and *ANAC096* expression is upregulated by forceps wounding after 24 h. Arrowheads indicate the boundaries of the wound site. Scale bar, 100 μm.

(C) Phloem reconnection of *erf114,115* and *anac071,096* mutants 1–10 days after grafting. The mean ± SEM from five experiments with 12–16 plants per time point per experiment is shown.

(D) Heatmap showing differentially expressed cell-wall-related genes during grafting of *erf114,115* and *anac071,096* mutants compared with Col-0 at 24 HAG.

(E) Expression pattern of *ERF115pro:GUS-GFP* in the primary root under various treatments for 24 h. Cellulase, 0.03%; pectinase, 0.03%; NAA, 0.2 μM. Scale bar, 100 μm.

(F) Relative expression levels of *ERF115* and *ANAC096* in intact or forceps wounded *PMEI5oe* after 24 h of wounding. Values are normalized by *PP2A* expression and represent the mean ± SEM of three to four experiments (n = 45–60 plants per experiment). Asterisks indicate statistically significant differences compared with Col-0 (Student's t test; ***p < 0.001).

(G) Expression pattern of *ERF115pro:GUS-GFP* in intact Col-0 and inducible *PMEI5* overexpression line (*iPMEI5oe*) roots. Boxplots represent the quantification of signal intensity. n = 14 for *ERF115pro:GUS-GFP* × Col-0, 18 for *ERF115pro:GUS-GFP* × *iPMEI5oe*. Asterisks indicate statistically significant differences compared with wild type (Wilcoxon test; ***p < 0.001). Scale bar, 50 μm.

See also Figure S6 and Data S2 and S3.

(Figures 5 and 6E). We also perturbed cell walls genetically and found strong *ERF115* and *ANAC096* induction in *PMEI5oe* and *kor1* intact plants compared with wild type but no changes in wounded plants (Figures 6F, 6G, and S6J). Introducing the negative repressor *ERF115-SRDX*[16] into the *PMEI5oe* background reduced the enhanced phloem reconnection rate of *PMEI5oe* (Figure S6K). Together, these data indicated that degradation or changes to cellulose and pectin were sufficient to induce wound-responsive ERFs and ANACs.

DISCUSSION

Here, we identified a group of four related DOF transcription factors that were activated early after wounding and promoted healing after grafting, hypocotyl pinching, callus formation, and stem incision. The dofQ mutant had no strong developmental defects in unwounded plants, but it significantly affected regeneration that required loss of all four DOFs, suggesting that they regulated similar processes. Grafting with dofQ affected the expression of genes related to cambium, phloem, and xylem, but notable was the perturbed induction of cell-wall-related genes. We noticed strong defects in graft attachment and callus formation in the dofQ mutant, which might be from an inability to dynamically regulate cell-wall composition relevant for early stages of tissue attachment and graft formation.[29,32] PME-related genes were upregulated in the dofQ rootstock (Figure S3F) and grafting with the *PMEI5oe* line in the rootstock enhanced graft formation (Figure 4C), hinting that enhanced PME activity below the graft junction might be inhibitory for healing. In addition, *CEL3*, whose homolog is important for successful inter-species grafts,[32] was regulated by DOFs and was a direct target of TMO6. Thus, increasing DOF levels and reducing PMEs could be an efficient means to improving graft formation and allowing a wider range of species to be grafted.

It has been previously shown that during vascular development, *HCA2*, *TMO6*, *DOF6*, and *DOF2.1* are expressed primarily in the vascular cylinder but with notable expression differences.[35,43] *DOF2.1* expresses in the xylem pole pericycle cells and adjacent endodermis and procambium,[43] whereas *HCA2*, *TMO6*, and *DOF6* express primarily in the protophloem

sieve elements and, for *HCA2* and *TMO6*, also in the procambium.[35,41] Upon wounding, we see strong vascular induction of all four transcriptional reporters, but *HCA2* and *TMO6* were exceptional since they also showed ectopic expression in the endodermis, cortex, and epidermis (Figures 1 and 2). *HCA2* and *TMO6* also showed strong expression above the cut but not below the cut when hypocotyls were left separated (Figure S1A), suggesting that *HCA2* and *TMO6* are highly responsive to a mobile signal that might also cause such ectopic expression. One such signal is likely auxin, since blocking auxin transport with NPA, inhibiting auxin receptor signaling with auxinole, or reducing auxin response with *iaa18-1* prevented *HCA2* and *TMO6* wound activation (Figure 5). However, adding auxin in the absence of wounding seemed to have little effect upon *HCA2* or *TMO6* induction, similar to previous reports that found *ERF115* induction by auxin in root tips required wounding.[6,7] Our findings, along with previous observations that *ERF115* did not require auxin or cell expansion for wound activation,[7] suggest that factor(s) other than auxin are used to recognize wounding.

Our data indicate that cell-wall damage is relevant since chemical or genetic perturbations to pectin and cellulose were sufficient to activate *HCA2* and *TMO6* (Figure 4). This activation occurred even when turgor pressure was reduced with mannitol treatment (Figures S4A and S4B),[7,27] suggesting that modifications to the cell walls themselves are a wound signal. Pectinase or cellulase treatments did not induce *HCA2* and *TMO6* expression without wounding, perhaps due to the inability of the enzymes to reach or damage the inner cell layers of the hypocotyl or root. However, perturbing cell walls using *PMEI5oe* and *kor1* modified DOF, ANAC, and ERF levels in wounded or unwounded plants. Previous studies have shown that *PMEI5oe* plants have increased pectin DM, reduced cell elongation, and increased cell-wall stiffness in elongating hypocotyls.[28] Both *PMEI5oe* and pectin digestion were sufficient to activate *HCA2* and *TMO6*, which seems counter-intuitive given their presumed opposite effects on cell-wall loosening. It could be that *PMEI5oe* cells are so stiff that growth results in self-inflicted wounding by shearing of the cell wall. Alternatively, pectinase treatment, wounding, and *PMEI5oe* might all increase pectin DM levels, which itself is a trigger for DOF induction. We also observed a close relationship between pectins and auxin as has been previously described in growing hypocotyls.[28] *TMO6* induction by pectinase and *PMEI5oe* enhancement of graft formation required auxin signaling (Figures 5A, 5B, S5A, S5B, and S5J), consistent with auxin acting downstream of pectin modifications. Thus, wound-induced pectin modifications to the cell wall could trigger an auxin response to promote DOF activation and regeneration. However, cellulase treatments behaved differently and did not appear to be auxin dependent, consistent with previous findings that auxin and cellulase treatments were additive for graft junction attachment.[29] Importantly, the pattern of *TMO6* induction by auxin or cellulase appeared non-overlapping: auxin induced *TMO6* close to the cut, whereas cellulase acted distally (Figure 5A). A combination of auxin and cellulase resulted in broad *TMO6* expression, suggesting that both processes contribute to induction. We propose that wounding modifies both the cellulose microfibrils and pectic matrix

polysaccharides to induce downstream genes, the DOFs, but do so via different mechanisms.

Our findings with DOFs appear to apply more broadly to other transcription factors involved in regeneration. Both *ERF115* and *ANAC096* were induced by changes to the pectin or cellulose—either genetically or chemically—but also had notable differences compared with *HCA2* and *TMO6*. It is known that *ERF115* is typically expressed in the QC and protoxylem cells, and upon vascular wounding, and its expression spreads outwards to the endodermis,[6] whereas cortex wounding causes ERF115 expression to activate inwards to the endodermis.[44] DOF expression did not show a clear inward or outward bias; instead, wounding caused expression to spread laterally and to adjacent cell layers similar to *ANAC096*.[15] Surprisingly, *ANAC096* and *ERF115* were highly upregulated in both unwounded *PMEI5oe* and *kor1* mutants suggesting that modifications to the pectin or cellulose were sufficient to activate *ANAC096* and *ERF115*. We also observed that DOFs, ANACs, and ERFs regulated multiple downstream targets related to cell-wall biology, including *CEL3*. Thus, our data are consistent with a common mechanism whereby damage to the pectin or cellulose induces DOFs, ANACs, and ERFs transcription factors and promotes tissue attachment, wound filling, vascular regeneration, and cell wall remodeling (Figure S6L). Such factors will be important for improving regeneration and also for elucidating the ligands and receptors that regulate wound perception.

STAR★METHODS

Detailed methods are provided in the online version of this paper and include the following:

- KEY RESOURCES TABLE
- RESOURCE AVAILABILITY
  - Lead contact
  - Material availability
  - Data and code availability
- EXPERIMENTAL MODEL AND SUBJECT DETAILS
- METHOD DETAILS
  - Plant material and transformation
  - Plant micro-grafting
  - Squeezing and cutting treatments
  - Microscopy
  - Laser-assisted cell ablation
  - RT-qPCR assays
  - Phylogenetic tree
  - Stem incision assays
  - Root phenotypes
  - Callus induction
  - Transcriptomic analyses
  - ChIP-qPCR assays
  - Cell-wall analysis
- QUANTIFICATION AND STATISTICAL ANALYSIS

SUPPLEMENTAL INFORMATION

Supplemental information can be found online at https://doi.org/10.1016/j.cub.2022.02.069.

AUTHOR CONTRIBUTIONS

A.Z. and C.W.M. conceived the experiments. A.Z., K.M., A.K., M.R., and M.A. performed the experiments. P.R., B.B., and A.B. generated materials. L.D.V., C.V., M.A., and C.W.M. supervised the experiments. A.Z. and C.W.M. wrote the paper. All authors edited and revised the final paper.

DECLARATION OF INTERESTS

The authors declare no competing interests.

REFERENCES

1. Miller, G., Schlauch, K., Tam, R., Cortes, D., Torres, M.A., Shulaev, V., Dangl, J.L., and Mittler, R. (2009). The plant NADPH oxidase RBOHD mediates rapid systemic signaling in response to diverse stimuli. Sci. Signal. *2*, ra45.

2. Toyota, M., Spencer, D., Sawai-Toyota, S., Jiaqi, W., Zhang, T., Koo, A.J., Howe, G.A., and Gilroy, S. (2018). Glutamate triggers long-distance, calcium-based plant defense signaling. Science *361*, 1112–1115.

3. Hander, T., Fernández-Fernández, Á.D., Kumpf, R.P., Willems, P., Schatowitz, H., Rombaut, D., Staes, A., Nolf, J., Pottie, R., Yao, P., et al. (2019). Damage on plants activates Ca²⁺-dependent metacaspases for release of immunomodulatory peptides. Science *363*, eaar7486.

4. Engelsdorf, T., Gigli-Bisceglia, N., Veerabagu, M., McKenna, J.F., Vaahtera, L., Augstein, F., Van der Does, D., Zipfel, C., and Hamann, T. (2018). The plant cell wall integrity maintenance and immune signaling systems cooperate to control stress responses in *Arabidopsis thaliana*. Sci. Signal. *11*, eaao3070.

5. Zhou, F., Emonet, A., Dénervaud Tendon, V., Marhavy, P., Wu, D., Lahaye, T., and Geldner, N. (2020). Co-incidence of damage and microbial patterns controls localized immune responses in roots. Cell *180*, 440–453.e18.

6. Canher, B., Heyman, J., Savina, M., Devendran, A., Eekhout, T., Vercauteren, I., Prinsen, E., Matosevich, R., Xu, J., Mironova, V., and De Veylder, L. (2020). Rocks in the auxin stream: wound-induced auxin accumulation and ERF115 expression synergistically drive stem cell regeneration. Proc. Natl. Acad. Sci. USA *117*, 16667–16677.

7. Hoermayer, L., Montesinos, J.C., Marhava, P., Benková, E., Yoshida, S., and Friml, J. (2020). Wounding-induced changes in cellular pressure and localized auxin signalling spatially coordinate restorative divisions in roots. Proc. Natl. Acad. Sci. USA *117*, 15322–15331.

8. Huot, B., Yao, J., Montgomery, B.L., and He, S.Y. (2014). Growth-defense tradeoffs in plants: a balancing act to optimize fitness. Mol. Plant *7*, 1267–1287.

9. Zhang, Y., and Turner, J.G. (2008). Wound-induced endogenous jasmonates stunt plant growth by inhibiting mitosis. PLoS One *3*, e3699.

10. Zhang, G., Zhao, F., Chen, L., Pan, Y., Sun, L., Bao, N., Zhang, T., Cui, C.X., Qiu, Z., Zhang, Y., et al. (2019). Jasmonate-mediated wound signalling promotes plant regeneration. Nat. Plants *5*, 491–497.

11. Asahina, M., Azuma, K., Pitaksaringkarn, W., Yamazaki, T., Mitsuda, N., Ohme-Takagi, M., Yamaguchi, S., Kamiya, Y., Okada, K., Nishimura, T., et al. (2011). Spatially selective hormonal control of RAP2.6L and ANAC071 transcription factors involved in tissue reunion in *Arabidopsis*. Proc. Natl. Acad. Sci. USA *108*, 16128–16132.

12. Matosevich, R., Cohen, I., Gil-Yarom, N., Modrego, A., Friedlander-Shani, L., Verna, C., Scarpella, E., and Efroni, I. (2020). Local auxin biosynthesis is required for root regeneration after wounding. Nat. Plants *6*, 1020–1030.

13. Pitaksaringkarn, W., Matsuoka, K., Asahina, M., Miura, K., Sage-Ono, K., Ono, M., Yokoyama, R., Nishitani, K., Ishii, T., Iwai, H., and Satoh, S. (2014). XTH20 and XTH19 regulated by ANAC071 under auxin flow are involved in cell proliferation in incised *Arabidopsis* inflorescence stems. Plant J. *80*, 604–614.

14. Matsuoka, K., Sugawara, E., Aoki, R., Takuma, K., Terao-Morita, M., Satoh, S., and Asahina, M. (2016). Differential cellular control by cotyledon-derived phytohormones involved in graft reunion of Arabidopsis hypocotyls. Plant Cell Physiol. *57*, 2620–2631.

15. Matsuoka, K., Sato, R., Matsukura, Y., Kawajiri, Y., Iino, H., Nozawa, N., Shibata, K., Kondo, Y., Satoh, S., and Asahina, M. (2021). Wound-inducible ANAC071 and ANAC096 transcription factors promote cambial cell formation in incised Arabidopsis flowering stems. Commun. Biol. *4*, 369.

16. Heyman, J., Cools, T., Vandenbussche, F., Heyndrickx, K.S., Van Leene, J., Vercauteren, I., Vanderauwera, S., Vandepoele, K., De Jaeger, G., Van Der Straeten, D., and De Veylder, L. (2013). ERF115 controls root quiescent center cell division and stem cell replenishment. Science *342*, 860–863.

17. Zhou, W., Lozano-Torres, J.L., Blilou, I., Zhang, X., Zhai, Q., Smant, G., Li, C., and Scheres, B. (2019). A jasmonate signaling network activates root stem cells and promotes regeneration. Cell *177*, 942–956.e14.

18. Kong, X., Tian, H., Yu, Q., Zhang, F., Wang, R., Gao, S., Xu, W., Liu, J., Shani, E., Fu, C., et al. (2018). PHB3 maintains root stem cell niche identity through ROS-responsive AP2/ERF transcription factors in *Arabidopsis*. Cell Rep. *22*, 1350–1363.

19. Heyman, J., Cools, T., Canher, B., Shavialenka, S., Traas, J., Vercauteren, I., Van den Daele, H., Persiau, G., De Jaeger, G., Sugimoto, K., and De Veylder, L. (2016). The heterodimeric transcription factor complex ERF115-PAT1 grants regeneration competence. Nat. Plants *2*, 16165.

20. Bou Daher, F., Chen, Y., Bozorg, B., Clough, J., Jönsson, H., and Braybrook, S.A. (2018). Anisotropic growth is achieved through the additive mechanical effect of material anisotropy and elastic asymmetry. eLife *7*, e38161.

21. Melnyk, C.W., Schuster, C., Leyser, O., and Meyerowitz, E.M. (2015). A developmental framework for graft formation and vascular reconnection in *Arabidopsis thaliana*. Curr. Biol. *25*, 1306–1318.

22. Peaucelle, A., Wightman, R., and Höfte, H. (2015). The control of growth symmetry breaking in the *Arabidopsis* hypocotyl. Curr. Biol. *25*, 1746–1752.

23. Chaudhary, A., Chen, X., Gao, J., Leśniewska, B., Hammerl, R., Dawid, C., and Schneitz, K. (2020). The Arabidopsis receptor kinase STRUBBELIG regulates the response to cellulose deficiency. PLoS Genet. *16*, e1008433.

24. Peng, L., Hocart, C.H., Redmond, J.W., and Williamson, R.E. (2000). Fractionation of carbohydrates in *Arabidopsis* root cell walls shows that three radial swelling loci are specifically involved in cellulose production. Planta *211*, 406–414.

25. Benedetti, M., Pontiggia, D., Raggi, S., Cheng, Z., Scaloni, F., Ferrari, S., Ausubel, F.M., Cervone, F., and De Lorenzo, G. (2015). Plant immunity triggered by engineered in vivo release of oligogalacturonides, damage-associated molecular patterns. Proc. Natl. Acad. Sci. USA *112*, 5533–5538.

26. Souza, C.A., Li, S., Lin, A.Z., Boutrot, F., Grossmann, G., Zipfel, C., and Somerville, S.C. (2017). Cellulose-derived oligomers act as damage-associated molecular patterns and trigger defense-like responses. Plant Physiol. *173*, 2383–2398.

27. Mielke, S., Zimmer, M., Meena, M.K., Dreos, R., Stellmach, H., Hause, B., Voiniciuc, C., and Gasperini, D. (2021). Jasmonate biosynthesis arising from altered cell walls is prompted by turgor-driven mechanical compression. Sci. Adv. *7*, eabf0356.

28. Jonsson, K., Lathe, R.S., Kierzkowski, D., Routier-Kierzkowska, A.L., Hamant, O., and Bhalerao, R.P. (2021). Mechanochemical feedback mediates tissue bending required for seedling emergence. Curr. Biol. *31*, 1154–1164.e3.

29. Kawakatsu, Y., Sawai, Y., Kurotani, K.I., Shiratake, K., and Notaguchi, M. (2020). An in vitro grafting method to quantify mechanical forces of adhering tissues. Plant Biotechnol. (Tokyo) *37*, 451–458.

30. Melnyk, C.W. (2017). Plant grafting: insights into tissue regeneration. Regeneration (Oxf) *4*, 3–14.

31. Melnyk, C.W., Gabel, A., Hardcastle, T.J., Robinson, S., Miyashima, S., Grosse, I., and Meyerowitz, E.M. (2018). Transcriptome dynamics at *Arabidopsis* graft junctions reveal an intertissue recognition mechanism that activates vascular regeneration. Proc. Natl. Acad. Sci. USA *115*, E2447–E2456.

32. Notaguchi, M., Kurotani, K.I., Sato, Y., Tabata, R., Kawakatsu, Y., Okayasu, K., Sawai, Y., Okada, R., Asahina, M., Ichihashi, Y., et al. (2020). Cell-cell adhesion in plant grafting is facilitated by beta-1,4-glucanases. Science *369*, 698–702.

33. Ramirez-Parra, E., Perianez-Rodriguez, J., Navarro-Neila, S., Gude, I., Moreno-Risueno, M.A., and Del Pozo, J.C. (2017). The transcription factor OBP4 controls root growth and promotes callus formation. New Phytol. *213*, 1787–1801.

34. Skirycz, A., Radziejwoski, A., Busch, W., Hannah, M.A., Czeszejko, J., Kwaśniewski, M., Zanor, M.I., Lohmann, J.U., De Veylder, L., Witt, I., and Mueller-Roeber, B. (2008). The DOF transcription factor OBP1 is involved in cell cycle regulation in *Arabidopsis thaliana*. Plant J. *56*, 779–792.

35. Miyashima, S., Roszak, P., Sevilem, I., Toyokura, K., Blob, B., Heo, J.O., Mellor, N., Help-Rinta-Rahko, H., Otero, S., Smet, W., et al. (2019). Mobile PEAR transcription factors integrate positional cues to prime cambial growth. Nature *565*, 490–494.

36. Wang, M., Yuan, D., Gao, W., Li, Y., Tan, J., and Zhang, X. (2013). A comparative genome analysis of PME and PMEI families reveals the evolution of pectin metabolism in plant cell walls. PLoS One *8*, e72082.

37. León, J., Rojo, E., and Sánchez-Serrano, J.J. (2001). Wound signalling in plants. J. Exp. Bot. *52*, 1–9.

38. Wolf, S., Mravec, J., Greiner, S., Mouille, G., and Höfte, H. (2012). Plant cell wall homeostasis is mediated by brassinosteroid feedback signaling. Curr. Biol. *22*, 1732–1737.

39. Lane, D.R., Wiedemeier, A., Peng, L., Höfte, H., Vernhettes, S., Desprez, T., Hocart, C.H., Birch, R.J., Baskin, T.I., Burn, J.E., et al. (2001). Temperature-sensitive alleles of RSW2 link the KORRIGAN endo-1,4-beta-glucanase to cellulose synthesis and cytokinesis in Arabidopsis. Plant Physiol. *126*, 278–288.

40. Vain, T., Crowell, E.F., Timpano, H., Biot, E., Desprez, T., Mansoori, N., Trindade, L.M., Pagant, S., Robert, S., Höfte, H., et al. (2014). The cellulase KORRIGAN is part of the cellulose synthase complex. Plant Physiol. *165*, 1521–1532.

41. Guo, Y., Qin, G., Gu, H., and Qu, L.J. (2009). Dof5.6/HCA2, a Dof transcription factor gene, regulates interfascicular cambium formation and vascular tissue development in *Arabidopsis*. Plant Cell *21*, 3518–3534.

42. Ploense, S.E., Wu, M.F., Nagpal, P., and Reed, J.W. (2009). A gain-of-function mutation in *IAA18* alters *Arabidopsis* embryonic apical patterning. Development *136*, 1509–1517.

43. Smet, W., Sevilem, I., de Luis Balaguer, M.A., Wybouw, B., Mor, E., Miyashima, S., Blob, B., Roszak, P., Jacobs, T.B., Boekschoten, M.,

44. et al. (2019). DOF2.1 controls cytokinin-dependent vascular cell proliferation downstream of TMO5/LHW. Curr. Biol. *29*, 520–529.e6.

44. Marhava, P., Hoermayer, L., Yoshida, S., Marhavý, P., Benková, E., and Friml, J. (2019). Re-activation of stem cell pathways for pattern restoration in plant wound healing. Cell *177*, 957–969.e13.

45. Imlau, A., Truernit, E., and Sauer, N. (1999). Cell-to-cell and long-distance trafficking of the green fluorescent protein in the phloem and symplastic unloading of the protein into sink tissues. Plant Cell *11*, 309–322.

46. Chen, S., Zhou, Y., Chen, Y., and Gu, J. (2018). fastp: an ultra-fast all-in-one FASTQ preprocessor. Bioinformatics *34*, i884–i890.

47. Kim, D., Langmead, B., and Salzberg, S.L. (2015). HISAT: a fast spliced aligner with low memory requirements. Nat. Methods *12*, 357–360.

48. Anders, S., Pyl, P.T., and Huber, W. (2015). HTSeq—a Python framework to work with high-throughput sequencing data. Bioinformatics *31*, 166–169.

49. Love, M.I., Huber, W., and Anders, S. (2014). Moderated estimation of fold change and dispersion for RNA-seq data with DESeq2. Genome Biol. *15*, 550.

50. Pauwels, L., De Clercq, R., Goossens, J., Iñigo, S., Williams, C., Ron, M., Britt, A., and Goossens, A. (2018). A dual sgRNA approach for functional genomics in *Arabidopsis thaliana*. G3 (Bethesda) *8*, 2603–2615.

51. Ritter, A., Iñigo, S., Fernández-Calvo, P., Heyndrickx, K.S., Dhondt, S., Shi, H., De Milde, L., Vanden Bossche, R., De Clercq, R., Eeckhout, D., et al. (2017). The transcriptional repressor complex FRS7-FRS12 regulates flowering time and growth in *Arabidopsis*. Nat. Commun. *8*, 15235.

52. Melnyk, C.W. (2017). Monitoring vascular regeneration and xylem connectivity in *Arabidopsis thaliana*. Methods Mol. Biol. *1544*, 91–102.

53. Ursache, R., Andersen, T.G., Marhavý, P., and Geldner, N. (2018). A protocol for combining fluorescent proteins with histological stains for diverse cell wall components. Plant J. *93*, 399–412.

54. Livak, K.J., and Schmittgen, T.D. (2001). Analysis of relative gene expression data using real-time quantitative PCR and the $2^{-\Delta\Delta C}$T method. Methods *25*, 402–408.

55. Czechowski, T., Stitt, M., Altmann, T., Udvardi, M.K., and Scheible, W.R. (2005). Genome-wide identification and testing of superior reference genes for transcript normalization in *Arabidopsis*. Plant Physiol. *139*, 5–17.

56. Gardiner, J., Sherr, I., and Scarpella, E. (2010). Expression of *DOF* genes identifies early stages of vascular development in *Arabidopsis leaves*. Int. J. Dev. Biol. *54*, 1389–1396.

57. Edgar, R.C. (2004). MUSCLE: multiple sequence alignment with high accuracy and high throughput. Nucleic Acids Res. *32*, 1792–1797.

58. Dereeper, A., Guignon, V., Blanc, G., Audic, S., Buffet, S., Chevenet, F., Dufayard, J.F., Guindon, S., Lefort, V., Lescot, M., et al. (2008). Phylogeny.fr: robust phylogenetic analysis for the non-specialist. Nucleic Acids Res. *36*, W465–W469.

59. Nagayama, T., Nakamura, A., Yamaji, N., Satoh, S., Furukawa, J., and Iwai, H. (2019). Changes in the distribution of pectin in root border cells under aluminum stress. Front. Plant Sci. *10*, 1216.

60. Iwase, A., Harashima, H., Ikeuchi, M., Rymen, B., Ohnuma, M., Komaki, S., Morohashi, K., Kurata, T., Nakata, M., Ohme-Takagi, M., et al. (2017). WIND1 promotes shoot regeneration through transcriptional activation of ENHANCER OF SHOOT REGENERATION1 in Arabidopsis. Plant Cell *29*, 54–69.

61. Iwase, A., Mitsuda, N., Koyama, T., Hiratsu, K., Kojima, M., Arai, T., Inoue, Y., Seki, M., Sakakibara, H., Sugimoto, K., and Ohme-Takagi, M. (2011). The AP2/ERF transcription factor WIND1 controls cell dedifferentiation in *Arabidopsis*. Curr. Biol. *21*, 508–514.

62. Tian, T., Liu, Y., Yan, H., You, Q., Yi, X., Du, Z., Xu, W., and Su, Z. (2017). agriGO v2.0: a GO analysis toolkit for the agricultural community, 2017 update. Nucleic Acids Res. *45*, W122–W129.

63. Shu, H., Nakamura, M., Siretskiy, A., Borghi, L., Moraes, I., Wildhaber, T., Gruissem, W., and Hennig, L. (2014). *Arabidopsis* replacement histone variant H3.3 occupies promoters of regulated genes. Genome Biol. *15*, R62.

64. Moreno-Romero, J., Santos-González, J., Hennig, L., and Köhler, C. (2017). Applying the INTACT method to purify endosperm nuclei and to generate parental-specific epigenome profiles. Nat. Protoc. *12*, 238–254.

65. Polko, J.K., Barnes, W.J., Voiniciuc, C., Doctor, S., Steinwand, B., Hill, J.L., Jr., Tien, M., Pauly, M., Anderson, C.T., and Kieber, J.J. (2018). SHOU4 proteins regulate trafficking of cellulose synthase complexes to the plasma membrane. Curr. Biol. *28*, 3174–3182.e6.

66. Voiniciuc, C., and Günl, M. (2016). Analysis of monosaccharides in total mucilage extractable from *Arabidopsis* seeds. Bio Protoc. *6*, e1801.

67. Voiniciuc, C., Dean, G.H., Griffiths, J.S., Kirchsteiger, K., Hwang, Y.T., Gillett, A., Dow, G., Western, T.L., Estelle, M., and Haughn, G.W. (2013). Flying saucer1 is a transmembrane RING E3 ubiquitin ligase that regulates the degree of pectin methylesterification in *Arabidopsis* seed mucilage. Plant Cell *25*, 944–959.

STAR★METHODS

KEY RESOURCES TABLE

REAGENT or RESOURCE	SOURCE	IDENTIFIER
Antibodies		
anti-GFP	Thermo Fisher Scientific	Cat#A-11120; RRID: AB_221569
IgG from rabbit serum	Sigma	Cat#15006
Bacterial and virus strains		
Agrobacterium tumefacien GV3101	N/A	N/A
Subcloning Efficiency DH5α Competent Cells	Thermo Fisher Scientific	Cat#18265017
Chemicals, peptides, and recombinant proteins		
Murashige and Skoog Medium (MS)	Duchefa Biochemie	Cat#M0222.0050
Plant agar	Duchefa Biochemie	Cat#P1001.1000
FastDigest NheI	Thermo Fisher Scientific	Cat#FD0973
Rifampicin	Duchefa Biochemie	Cat#R0146.0001
Spectinomycin	Duchefa Biochemie	Cat#S0188.0005
Carboxyfluorescein diacetate (CFDA)	Biotium	Cat#51014
Dexamethasone	Sigma	Cat#D4902
β-Estradiol	Sigma	Cat#E8875
1-Naphtaleneacetic acid (NAA)	Sigma	Cat#N0640
1-N-Naphthylphthalamic acid (NPA)	Sigma	Cat#33371
Auxinole	MedChemExpress	Cat#HY-111444
Salicylic acid	Sigma	Cat#S0875
Methyl jamonate	Sigma	Cat#392707
Driselase	Kyowa Hakko Kogyo	LotKY4060
Pectinase	Sigma	Cat#P2401
Cellulase	Calbiochem	Cat#219466
D-Mannitol	VWR	Cat#25311.366
DMSO	Sigma	Cat#276855
Urea	Sigma	Cat#U5378
Sodium deoxycholate	Sigma	Cat#30970
Xylitol	Sigma	Cat#X3375
Calcofluor White	Sigma	Cat#F3543
Propidium iodide	Sigma	Cat#P4864
Paraformaldehyde	Sigma	Cat#158127
Potassium Ferricyanide ($K_3Fe(CN)_6$)	Sigma	Cat#60279
Potassium Ferrocyanide ($K_4Fe(CN)_6$)	Sigma	Cat#P9387
X-Gluc	Thermo Fisher Scientific	Cat#R0851
Sodium phosphate dibasic dodecahydrate ($Na2HPO4$)	Sigma	Cat#04273
Sodium phosphate dibasic dihydrate ($NaH2PO4$)	Sigma	Cat#71645
Glycerol	Sigma	Cat#49781
NaCl	Duchefa Biochemie	Cat#65827
Triton X-100	Sigma	Cat#T8787
Formaldehyde	Sigma	Cat#F8775
Glycine	VWR	Cat#1.04201.1000
Hexylene glycol	Sigma	Cat#112100

Continued

REAGENT or RESOURCE	SOURCE	IDENTIFIER
Piperazin-1,4-bis(2-etansulfonsyra) buffertsubstans, PIPES	Sigma	Cat#1.10220.0250
MgCl₂	Merck	Cat#1058330250
EGTA	Sigma	Cat#E4378
KCl	Sigma	Cat#A2939
cOmplete, Mini, EDTA-free Protease Inhibitor Cocktail	Roche	Cat# 11836170001
2-mercaptoethanol	Sigma	Cat#M6250
TRIS	VWR	Cat#28811.364
Ethylenediaminetetraacetic acid disodium salt dihydrate	Merck	Cat#ED2SS
Sodium dodecyl sulfate (SDS)	Sigma	Cat#05030
NaHCO₃	Sigma	Cat#372382
Dynabeads Protein A for Immunoprecipitation	Invitrogen	Cat#10001D
Ruthenium red	Sigma	Cat# R2751
GelRite	Duchefa Biochemie	Cat# G1101.1000
MES monohydrate	Duchefa Biochemie	Cat#M1503.0250
HYGROMYCINE B	MES monohydrate	Cat#H0192.0001
Basta (Glufosinate-ammonium)	Sigma	Cat#45520
Critical commercial assays		
Roti-Prep RNA MINI	ROTH	Cat#8485.3
Maxima First Strand cDNA Synthesis Kit	Thermo Fisher Scientific	Cat#K1642
Maxima SYBR Green/ROX qPCR Master Mix (2X)	Thermo Fisher Scientific	Cat#K0222
IPure Kit v2	Diagenode	Cat#C03010014
NEBNext Poly(A) mRNA Magnetic Isolation Module	New England Biolabs	Cat# E7490S
NEBNext Ultra II RNA Library Prep Kit for Illumina	New England Biolabs	Cat#E7770S
NEBNext Multiplex Oligos for Illumina (Dual Index Primers Set 1)	New England Biolabs	Cat#E7600S
Qubit RNA HS Assay Kit	Thermo Fisher Scientific	Cat#Q32855
Agilent DNA 1000 Kit	Agilent	Cat#5067-1504
Deposited data		
Transcriptomics datafiles	Gene Expression Omnibus	GEO: GSE179283
Experimental models: Organisms/strains		
Arabidopsis: Col-0	N/A	N/A
Arabidopsis: *tmo6-4*	Miyashima et al.[35]	N/A
Arabidopsis: *hca2*	Miyashima et al.[35]	GK-466B10
Arabidopsis: *dof2.1-1*	Smet et al.[43]	GK-668G12
Arabidopsis: *dof6-1*	Miyashima et al.[35]	Wiscseq_Ds_Llox351c08
Arabidopsis: *HCA2-SRDX*	Guo et al.[41]	N/A
Arabidopsis: *hca2-OE*	Guo et al.[41]	N/A
Arabidopsis: *tmo6-4,dof6-1*	Miyashima et al.[35]	N/A
Arabidopsis: *hca2,tmo6-2*	this study	N/A
Arabidopsis: *tmo6-1,dof2.1-2,dof6-2*	Smet et al.[43]	N/A
Arabidopsis: *hca2,tmo6-4,dof6-1*	this study	N/A
Arabidopsis: *hca2,tmo6-4,dof2.1-1,dof6-1*	this study	N/A
Arabidopsis: pear sextuple (*pear1,pear2,dof6-1,tmo6-4, hca2,obp2*)	Miyashima et al.[35]	N/A
Arabidopsis: *erf115*	Heyman et al.[16]	SALK_021981
Arabidopsis: *erf114,115*	this study	N/A

(Continued on next page)

Continued

REAGENT or RESOURCE	SOURCE	IDENTIFIER
Arabidopsis: ERF115-SRDX	Heyman et al.[16]	N/A
Arabidopsis: anac071,096	Matsuoka et al.[14]	N/A
Arabidopsis: Ler	N/A	N/A
Arabidopsis: iaa18-1 (Ler)	Ploense et al.[42]	N/A
Arabidopsis: PMEIoe	Wolf et al.[38]	N/A
Arabidopsis: iPMEIoe	Wolf et al.[38]	N/A
Arabidopsis: kor1-4	Mielke et al.[27]	N/A
Arabidopsis: kor1-6	Mielke et al.[27]	SALK_075812
Arabidopsis: cel3-2	Notaguchi et al.[32]	CS_803355
Arabidopsis: CRE1[XVE]$_{pro}$:TMO6	Miyashima et al.[35]	N/A
Arabidopsis: CRE1[XVE]$_{pro}$:HCA2	Miyashima et al.[35]	N/A
Arabidopsis: CRE1[XVE]$_{pro}$:DOF6	Miyashima et al.[35]	N/A
Arabidopsis: RPS5A$_{pro}$:DOF2.1-GR	Smet et al.[43]	N/A
Arabidopsis: TMO6$_{pro}$:erRFP	Miyashima et al.[35]	N/A
Arabidopsis: HCA2$_{pro}$:erRFP	Melnyk et al.[31]	N/A
Arabidopsis: DOF2.1$_{pro}$:GUS-GFP	Smet et al.[43]	N/A
Arabidopsis: DOF6$_{pro}$:erVENUS	Smet et al.[43]	N/A
Arabidopsis: ERF115$_{pro}$:GUS-GFP	Heyman et al.[19]	N/A
Arabidopsis: ANAC096$_{pro}$:GUS	Matsuoka et al.[14]	N/A
Arabidopsis: TMO6$_{pro}$:TMO6-YFP	Miyashima et al.[35]	N/A
Arabidopsis: SUC2$_{pro}$:GFP	Imlau et al.[45]	N/A
Oligonucleotides		
Table S2	N/A	N/A
Recombinant DNA		
pDE_Cas9_TMO6C (HygR)	Miyashima et al [35]	N/A
pDE_CAS9_ERF114 (BastaR)	this study	N/A
Software and algorithms		
R version 3.6.2	N/A	https://www.r-project.org/
Microsoft Excel v16.54	Microsoft	N/A
Affinity Photo v1.10.4	Affinity	N/A
Fiji v2.0.0	N/A	https://fiji/sc/
Zeiss Zen Black 2.3 SP1	Zeiss	https://www.zeiss.com/
Zeiss Zen Blue 2.3 lite and 2.5	Zeiss	https://www.zeiss.com/
Lecia Apllication Suite X (LAS X)	Lecia Microsystems	https://www.leica-microsystems.com/
SnapGene 5.2	N/A	https://www.snapgene.com/
Fastp	Chen et al.[46]	N/A
hisat2	Kim et al.[47]	N/A
Htseq	Anders et al.[48]	N/A
DESeq2 package	Love et al.[49]	N/A
Ggplot2 package	N/A	https://www.r-project.org/
Other		
Zeiss LSM780 confocal microscope	Zeiss	https://www.zeiss.com/
Zeiss Axioscope A1	Zeiss	https://www.zeiss.com/
Leica M205 FA stereo-fluorescent microscope	Lecia Microsystems	https://www.leica-microsystems.com/
Qubit 2.0 Fluorometer	Invitrogen	N/A
Agilent 2100 Bioanalyzer	Agilent	N/A
Bioruptor	Diagenode	N/A

RESOURCE AVAILABILITY

Lead contact
Further information and requests for regents and resources should be directed to and will be fulfilled by Charles W. Melnyk (charles.melnyk@slu.se).

Material availability
All unique/stable reagents generated in this study are available from the lead contact without restriction.

Data and code availability
The Gene Expression Omnibus (GEO) accession number for the transcriptomic data reported in this paper is GEO: GSE179283. The transcriptomic data is available from GEO or the lead contract upon request. This study did not generate original code.

EXPERIMENTAL MODEL AND SUBJECT DETAILS

Arabidopsis thaliana ecotype Columbia-0 (Col-0) was used as the wild type in this study, except where indicated. Mutants and transgenic lines are detailed as key resources table. For genotypes observed in F1, phenotypes were compared to F1s (parent x Col-0). Seeds were surface sterilized with 75% (v/v) ethanol for 20 minutes, then 99.5% (v/v) ethanol for 5 minutes. The seeds were put in a sterile hood to remove residual ethanol. Sterilized seeds were then sown on half-strength Murashige and Skoog (MS) medium with 1% (w/v) plant agar. After 2 days of stratification at 4 degrees (°C), seeds were moved to the growth chamber (8 hours of light/16 hours of dark, ~110 μmol m^{-2} s^{-1}, 20°C, Conviron A1000 chamber). All plants were grown vertically.

METHOD DETAILS

Plant material and transformation
To create the *tmo6-2,hca2* mutant, the pDE_Cas9_TMO6C vector was transformed into the *hca2* mutant[35] line using floral dip transformation. Cas9 free and homozygous mutants were selected via hygromycin and NheI[35] in the T3 generation for further use. To make the *tmo6-4,hca2,dof6-1* and *tmo6-4,hca2,dof2.1-1,dof6-1* mutants, cross-pollination was performed between the previously published pear sextuple mutant[35] and the *dof2.1-1* mutant[43] and mutants confirmed by PCR. To make the *erf114,115* mutant, an *ERF114* CRISPR-Cas9 transgene was created using a dual guide RNA approach.[50] A construct targeting two different sites in the *ERF114* gene was designed where the single guide RNA (sgRNA), sgRNA1 and sgRNA2 were annealed and inserted via a cut ligation method using BbsI in pMR217_pDONR_P1P and pMR218_pDONR_P5P, respectively. Using a Gateway LR reaction, the two sgRNAs were combined in a destination vector pDE_CAS9_Basta.[51] The *erf114,115* mutant was obtained by transforming the *ERF114* CRISPR-Cas9 construct into the previously published *erf115* mutant[16] by floral dip transformation. Primary transformants were selected on agar plates containing Basta (10 mg/ml) and genotyped for the 235bp deleted fragment and further confirmed using Sanger sequencing. Genotyping primers are provided in Table S2.

Plant micro-grafting
7-day-old seedlings were used for micro-grafting and grafting assays were performed according to a previously published method.[52] Briefly, for attachment assays, grafted plants were picked up with forceps at the root and hypocotyl junction site. If the scion remained attached during the manipulation, the plant was considered attached. For the phloem connection assay, the cotyledon was damaged with forceps and carboxyfluorescein diacetate (CFDA) was dropped on the wound site. After 1 hour, phloem was considered reconnected if the fluorescent signal appeared in the root. New plants were used for each time point. For the xylem connection assay, the root 1-2cm below the hypocotyl was removed, then CDFA was dropped on the wound site. After 20 minutes, xylem was considered reconnected if the fluorescent signal was found in the cotyledon. For root growth assays, the presence of lateral roots growing from the grafted rootstock was scored. New plants were used for each time point. To observing phloem connection on the same plants over several days, a wild type scion expressing GFP in the phloem companion cell (*SUC2_{pro}:GFP*)[45] was grafted to various genotypes and GFP movement monitored in the root. To test the inducible lines during grafting, plants were treated with 10 μM estradiol or 10 μM dexamethasone (DEX) from germination until checking the connection efficiency. The fluorescent signal was monitored with a Leica M205 FA stereofluorescent microscope fitted with a YFP filter.

Squeezing and cutting treatments
6-day-old seedlings were gently squeezed with forceps in the mid hypocotyl region or cut in the mid hypocotyl region and placed on ½ MS agar plates containing various chemicals: NAA, 0.2 μM; NPA, 5 μM; auxinole, 30 μM; salicylic acid, 2 μM; methyl jamonate, 5 μM; mannitol, 0.23 M; Driselase, 0.03%, w/v; pectinase, 0.03%, w/v; cellulase, 0.03%, w/v.

Microscopy

For imaging the root tips of fluorescent reporter lines, Calcofluor White staining of the cell wall was performed according to Ursache et al.[53] For the analysis of vascular cell number, the root was mounted in 5 μM propidium iodide solution and imaged. Fluorescent images of whole-mount and hand-sectioned graft junctions were taken on an LSM-780 confocal microscope. For reporter lines expressing erRFP, 561 nm excitation and 580-625 nm emission were used. For reporter lines expressing GFP and erVENUS, 488 nm excitation and 500-527 nm emission were used. Z-stack projections were taken under non-saturating conditions. Fiji software was used to process images and quantify the average fluorescence intensity. For longitudinal images of hypocotyls from *TMO6pro:erRFP* and *HCA2pro:erRFP*, z-stack projections are shown and made using the average intensity and red hot Look Up Table (LUT) functions with Fiji. For longitudinal images of squeezed hypocotyls from *DOF2.1pro:GUS-GFP, DOF6pro:erVENUS* and *ERF115pro:GUS-GFP*, z-stack projections are shown and made using the average intensity and green LUT functions with Fiji. For longitudinal images of hypocotyls from *DOF2.1pro:GUS-GFP, DOF6pro:erVENUS* and *ERF115pro:GUS-GFP*, single planes are shown and made using the green LUT function with Fiji. GUS staining was performed according to a previously published method with minor modifications.[11] Forceps wounded and non-wounded plants were immersed in X-Glu solution (1 mg/mL) and incubated at 37°C for 12 hours. Samples were visualized with a Zeiss Axioscope A1 microscope.

Laser-assisted cell ablation

Cell-specific ablation experiments were performed with two-photon laser (MaiTai, SpectraPhysiscs) at an excitation wavelength of 735 nm at 80% laser power using 20x objective with a Zeiss LSM780 confocal microscope. The specific cell was ablated after selecting the region of interest (ROI). For longitudinal images of hypocotyls from *TMO6pro:erRFP* and *HCA2pro:erRFP*, single planes are shown and made using the red LUT function with Fiji. For the movie of root from *TMO6pro:erRFP*, a z-stack projection is shown and made using the red LUT function with Fiji. For longitudinal images of hypocotyls from *DOF2.1pro:GUS-GFP* and *DOF6pro:erVENUS*, single planes are shown and made using the green LUT function with Fiji.

RT-qPCR assays

Wound induction assay: 6-day-old seedlings were squeezed at several positions across the hypocotyl and root for the wounded treatment; intact control plants were not squeezed. 24 hours after wounding, intact and wounded plants were harvested but cotyledons removed. Total RNA was isolated using a Roti-Prep RNA MINI Kit. RNA samples were quantified using a NanoDrop ND-1000 spectrometer (Thermo Fisher Scientific). cDNA was prepared from 500 ng of total RNA using Maxima First Strand cDNA Synthesis Kit containing oligo(dT)$_{18}$ and random hexamer primers. The cDNA was diluted 1:9 with nuclease-free water. qPCR was performed using the iCycler iQ Real-Time PCR detection system with a 10 μL reaction volumes (5μL of 2X Maxima SYBR Green qPCR/ROX Master Mix, 0.75 μM of forward and reverse primers, and 2 μL of diluted cDNA). The following program was used for the qRT-PCR analysis: initial denaturation 95°C for 10 mins, 40 cycles of 95°C for 10 sec, 60°C for 30 sec and was followed by melt curve analysis to confirm the absence of off target amplification. Relative expression levels of selected genes were calculated using $2^{-\Delta\Delta CT}$ method.[54] *At1g13320*, the gene encoding protein phosphatase 2A subunit (*PPA2*), was used as a loading reference.[55] Three to five biological replicates were prepared for each genotype. Gene expression analyses in incised stems was performed as previously described.[11,15] Briefly, segments of flowering stems (from ~8 plants) were harvested. Total RNA was extracted using QIAshredder (Qiagen) and the RNeasy Plant Mini Kit (Qiagen) according to the manufacturer's instructions. cDNA was prepared from 1 μg of total RNA using the PrimeScript RT Reagent Kit with gDNA Eraser (Takara), and qPCR were performed using a 7500 Fast Real-Time PCR system (Thermo Fisher Scientific) with a 20 μL total reaction volume (10 μL of Fast SYBR Green Master Mix (Thermo Fisher Scientific), 1 μL of cDNA and 0.2 μM each primer). *ACT2* was the reference gene and three independent replicates were used. A list of primers used for RT-qPCR is provided in Table S2.

Phylogenetic tree

36 members of the DOF transcription factor family were used for a phylogenetic analysis.[56] The full protein sequences were aligned by MUSCLE with default setting.[57] Then the neighbor-joining (NJ) tree was generated, which were supported by 1000 replicates of bootstrap.[58]

Stem incision assays

Stem incision assays were performed as previously described[11,15] with several modifications. Briefly, flowering stems at 7 days after incision were harvested and fixed in a mixture of 1% (w/v) paraformaldehyde and 2.5% (v/v) glutaraldehyde in 0.1 M phosphate buffer (pH 7.4) overnight at 4°C. After washing with phosphate buffer, samples were embedded with Super Cryoembedding Medium (Section Lab, Hiroshima, Japan). The frozen block was mounted on a holder, and longitudinal cryosections (15 μm thick) were prepared with adhesive film (Cryofilm type 3C (16UF), Section Lab) using a cryostat (CM1860, Leica Microsystems, Wetzlar, Germany). Photographs of sections were captured using Scanscope CS2 scanner (Leica) after staining with 0.1% (w/v) toluidine blue O solution.

Root phenotypes

For root lengths, 5-day-old seedlings were transferred to mock, pectinase, and cellulase containing plates. Pictures were taken after 5 days of treatment. All plants were growth under long-day conditions (16 hours of light/8 hours of dark, ~110 μmol m^{-2} s^{-1}, 22°C, Conviron A1000 chamber). Fiji software was used to measure root lengths. For ruthenium red staining, 7-day-old seedlings were

briefly saponified with 0.1 N NaOH, which can remove methyl esters to facilitate ruthenium red binding of pectin glycosyl residues. Then, the seedlings were immerged in the 0.01% ruthenium red solution for 5 minutes.[59] Images were taken using a Zeiss Axioscope A1 microscope. Images were quantified using Fiji.

Callus induction

Callus induction from petiole explants was performed according to a previously published method with minor modifications.[60] Petioles were excised from 10-day-old seedlings which were grown under long-day conditions, then explants were cultured on MS medium supplemented with 1% sucrose and 0.6% Gelrite. Callus induction from hypocotyl explants was performed according to a previously published method with minor modifications.[61] The seeds were grown on MS medium supplemented with 0.05% MES, 0.5% Sucrose, 0.8% Gelrite and grown in the dark to induce etiolation. After 7 days, a cut was performed at approximately 7mm above the hypocotyl-root junction to induce callus. After 8 days induction, sample tissues were imaged with a Leica M205 FA stereo-fluorescent microscope. Projected callus area in the image were measured by the freehand tool in Fiji.

Transcriptomic analyses

Sample preparation was performed according to a previously published study.[31] After 24 hours of grafting, approximately 0.5mm of tissue was taken above or below the graft junction to prepare scion and rootstock samples. 1mm of tissue from intact non-grafted plants was also harvested. Each sample has three biological replicates and approximately 80 plants were harvested and combined per sample. Total RNA was isolated using a Roti-Prep RNA MINI Kit following the manufacturer's instructions. For RNAseq library preparation, 200ng of total RNA was treated using a Poly(A) mRNA Magnetic Isolation Module kit. The library was prepared with the resulting mRNA using a NEBNext Ultra II kit and NEBNext Multiplex Oligos for Illumina. Libraries were sequenced at Novogene on a NovaSeq 6000 in 150bp paired-end mode.

For RNAseq analyses, the raw data were filtered to remove the low quality of reads using fastp.[46] The cleaned reads were mapped to the *Arabidopsis* reference TAIR10 using hisat2.[47] The number of reads was counted using htseq.[48] Differentially expressed genes (DEG) were identified using the DESeq2 R package[49] and had a q-value < 0.05. Genes with a q-value < 0.05 were considered to have statistically significant expression differences between samples. In each tissue sample comparison, wild type Col-0 was the reference. The read counts for each gene were converted to TPM values using the previously described customized R script.[31] Gene ontology (GO) annotation was performed using agriGO.[62] The enrichment GO terms were determined with an adjusted p value < 0.05 (Chi-square test) and enrichment foldchange > 2. The lists of DEGs and GO annotations are provided in Data S1, S2, and S3 and Table S1. Previously published grafting time course RNAseq datasets in wild type Col-0 plants were analyzed from Melnyk et al.[31]

ChIP-qPCR assays

TMO6_{pro}:TMO6-YFP[35] plants were selected to test *CEL3* promoter interactions under wounded conditions. *TMO6_{pro}:TMO6-YFP* plants were squeezed with forceps at several points on roots and hypocotyls of 7-day-old seedling. After 24 hours of induction, we collected approximately ∼150mg seedling (∼1500 plants) for chromatin immunoprecipitation (ChIP). Non-transgenic Col-0 was used as a negative control. ChIP was performed according to a previously described protocol with minor modifications.[63,64] Briefly, plants were treated with 1% (v/v) formaldehyde in PSB solution under vacuum for two periods of 10 min, with a vacuum release between each period. Crosslinking was quenched by adding 0.125M glycine with another 5 min of vacuum infiltration. Nuclei were extracted using MEB buffer. Sonication was performed for 10x 20 sec "ON", 45 sec "OFF" cycles (high power) in a Bioruptor. Overnight antibody binding was performed directly after sonication, followed by the addition of washed protein A Dynabeads to each ChIP aliquot. De-crosslinking and subsequent DNA isolation were performed using the Ipure kit v2 following the manufacturer's instructions, after which qPCR was performed. Antibodies used in ChIP were anti-GFP and IgG as a mock control. All the experiments were performed with three biological replicates. For the qPCR data, we normalized the immunoprecipitation to IgG to obtain the fold enrichment of the target. qPCR primers are listed in Table S2.

Cell-wall analysis

For all the cell-wall biochemical analyses, 7-day-old seedlings were gently squeezed at several positions across the hypocotyl and root for the wounded treatment; intact control plants were not squeezed. 48 hours after wounding, intact and wounded plants were harvested but cotyledons removed. Approximately 1000-1500 seedlings were collected for each sample, yielding 12–31 mg of lyophilized tissue for each. Alcohol-insoluble residue (AIR) was prepared essentially as previously described,[65] starting with ball mill homogenization and sequent 70% ethanol, chloroform: methanol (1:1 v/v), and acetone washes. The dry AIR was carefully weighed and used to prepare homogeneous 1 mg/mL AIR slurry solutions in water that were aliquoted for the different analyses. The matrix polysaccharide composition of 300 μg AIR was determined after 2 M trifluoroacetic acid hydrolysis using high-performance anion-exchange chromatography coupled with pulsed electrochemical detection (HPAEC-PAD). All steps were performed as previously described,[66] except that Ribose internal standard was only added immediately before injection into the instrument and eluent setup detailed in Mielke et al.[27] Crystalline cellulose content was quantified following two-step sulfuric acid hydrolysis and HPAEC-PAD analysis, exactly as previously described.[27] Pectin DM was quantified as previously described,[67] but starting with 1 mg of dry AIR per sample for the 0.25 M NaOH saponification reaction. After neutralization with 0.25 M HCl and centrifugation, methanol released in the supernatant was quantified relative to standards using the previously described alcohol oxidase reaction to monitor changes in

absorbance at 412 nm.[67] The nmol of methanol normalized to the AIR content was divided by the nmol of GalA (from the HPAEC-PAD data) to calculate the relative pectin DM.

QUANTIFICATION AND STATISTICAL ANALYSIS

Student's t test was obtained using Excel (version 16.54). The Wilcoxon signed-rank test and ANOVA analysis were obtained using R (version 3.6.2). To determine statistical significance, independent Student's t tests with two-tail distribution between two groups and one-way ANOVA followed Tukey HSD test among various groups was used. The p values < 0.05 were considered to be statistically significant.